Reflection component based color similarity

Michael Hild
Osaka Electro-Communication University,
Dept. of Engineering Informatics
Neyagawa, Osaka, Japan

Abstract

We propose several new reflection component based color similarity measures and report on the results of an evaluation of their class separation ability, for which more than 50 test images (for facial skin color classification) have been used. It was found that two of the proposed color similarity measures (S_{13} and S_{14}) are superior.

1. Introduction

Color is a major source of visual information. It plays an important role in image retrieval [1, 2], image region segmentation [4, 3], and image based object tracking and recognition [5, 2, 3]. In these processes the major use of color is as a feature in color classification and determination of regions of homogeneous color. Since the essence of these processes is the forming of groups of pixels of *similar color*, the concept of *color similarity* is important. The implementation of this concept as a computational method leads us to the definition of *color similarity measures* (or CSMs, for short).

Many CSMs have been defined, and most of these definitions are based on the notion that a color is represented as a point (or vector) in a color space and that the similarity between two colors can be computed with these two color vectors as input. [8] However, if we want to apply CSMs to photographs and digital images of real scenes, CSM definitions based on the color point notion are no longer adequate, because the properties of the reflecting surfaces are neglected.

Reflections from surfaces of inhomogeneous dielectric materials can be described by the dichromatic reflection model, which states that reflections consist of two components, one due to diffuse reflection and the other due to specular reflection. [6, 7] When the reflections are picked up by sensor systems that integrate the visual spectrum over a finite number of separate spectral bands, the color of each pixel can be represented as a point in a finite-dimensional color space. The color points due to all pixels of an uniformly colored surface form two distinct clusters in the color space, one of them representing the diffuse reflection component and the other one representing the specular reflection component. Thus, color similarity in this case is not a matter of similarity between pairs of color points, but rather a matter of similarity between pairs of color point clusters, and color similarity measures must be defined accordingly.

Defining CSMs which are able to account for both the diffuse and specular reflection components, and applying them to general imagery is complicated. In order to simplify matters, we could define CSMs which determine similarity only between the diffuse reflection components. This seems justified because the characteristic "body" color of surfaces is mediated through the diffuse reflection component, whereas the specular reflection component only mediates the color of the illuminant, and for classification tasks we are mainly interested in finding matches between body colors.

In the main part of this paper we first show that existing CSMs are not adequate for computing diffuse reflection component based color similarity and we propose several new diffuse reflection component based color similarity measures. We report on evaluation results regarding the class separation ability of these CSMs, which were obtained from an experiment involving more than fifty test images used for solving a human (facial) skin color classification task. The test images depict real-world scenes shot with CCD cameras at a wide variety of outdoor and indoor locations.

2. Existing color similarity measures

One of the properties of diffuse reflection component based CSMs is their independence of the colors' brightness values. That is, when computing the color similarity between a given reference color and a set of colors sampled from a homogeneously colored surface on which the luminance of surface points varies with the points' locations, a diffuse reflection based CSM will return the same similarity value for all points on that surface. CSMs with this property do already exist and are described in the literature [8]. Three such CSMs are defined as follows:

Measure 1

$$S_1 = \frac{\mathbf{x}_i \cdot \mathbf{x}_j}{\| \mathbf{x}_i \| \cdot \| \mathbf{x}_j \|} = \cos(\theta) \qquad (1)$$

where θ is the angle between vectors $\mathbf{x}_i$ and $\mathbf{x}_j$.

Measure 3

$$S_3 = \frac{\| \mathbf{x}_i \| \cos(\theta) + \| \mathbf{x}_j \| \cos(\theta)}{(\| \mathbf{x}_i \|^2 + \| \mathbf{x}_j \|^2 + 2 \| \mathbf{x}_i \| \| \mathbf{x}_j \| \cos(\theta))^{\frac{1}{2}}} \quad (2)$$

Measure 4

$$S_4 = \frac{\cos(\theta) \left(\| \mathbf{x}_i \|^2 + \| \mathbf{x}_j \|^2 + 2 \| \mathbf{x}_i \| \| \mathbf{x}_j \| \cos(\theta)\right)^{\frac{1}{2}}}{\| \mathbf{x}_i \| + \| \mathbf{x}_j \|} \quad (3)$$

These CSMs take two color vectors as input and compute a real number in the range (0.0, 1.0), where value 1.0 indicates "identical" and "0.0" is synonymous with "not similar at all." They are represented as functions $S_k(\mathbf{x}_i, \mathbf{x}_j)$, where $\mathbf{x}_i, \mathbf{x}_j$ are the two p-dimensional color vectors. [1]

The above formulae are all given for p-dimensional color vectors; i.e., they are not limited to the three spectral channels implemented in most contemporary CCD cameras. The components of these vectors are obtained by integrating filtered reflection spectra over the visual wavelength range such as

$$x_{ik} = \int_{\lambda_1}^{\lambda_2} E(\lambda) S(\lambda) F_k(\lambda) d\lambda \quad (4)$$

where $E(\lambda)$: illumination, $S(\lambda)$: spectral reflectance function, $F_k(\lambda)$: k-th filter function, (λ_1, λ_2): range of visual spectrum wavelengths, and
$\mathbf{x}_i = (x_{i1} \quad x_{i2} \quad \ldots \quad x_{ik})^T$: the i-th color vector. However, since practically all commercially available cameras come with the three (R,G,B) channels, we carry out all experiments in this paper for the RGB color space.

Color is a vector-valued signal of at least three dimensions, whereas the feature being generated through the application of color similarity measures is a scalar. Thus, color similarity measures implement a mapping from the p-dimensional color space to a one-dimensional (scalar) space. Given a reference color, a CSM assigns a scalar value between 0 and 1 to all other colors of the color space; in this way CSMs superimpose a scalar field on the color space, the structure of which depends on the reference color and the mathematical definition of the CSMs. It is important to realize that some mathematical formulations of CSMs are superior in terms of class separation ability.

The spatial structure of CSMs can be made explicit by computing (hyper-) surfaces of constant similarity with respect to the reference color, and conclusions about the properties of CSMs can be drawn by examining the size and form of such surfaces. The diagram of the constant-similarity surface for the S_1–CSM is shown in Fig.1. This diagram was computed by setting the reference color to $\mathbf{x}_i = (128 \quad 128 \quad 0)^T$ (i.e. pure yellow of medium brightness) and searching for all colors $\mathbf{x}_j$ that satisfy $0.80 \leq S_k(\mathbf{x}_i, \mathbf{x}_j) \leq 0.81$. The obtained color points then were linked by straight line segments and displayed as a surface. The constant-similarity surfaces for the S_3– and S_4–CSMs are very similar.

This diagram shows that the *extent over color space* of the constant-similarity surfaces of the three CSMs is very wide. Due to this "low compactness", the measures S_1, S_3 and S_4 are unlikely to perform well in the context of color classification tasks.

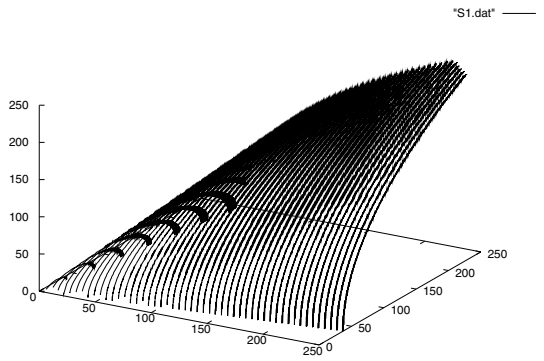

Figure 1: *Constant similarity surface for* $S_1 = 0.8$

3. Reflection component based color similarity measures

Since the three existing diffuse reflection component based CSMs lack compactness, better CSMs need to be defined.

3.1. A new set of diffuse reflection component based CSMs

In this section we propose and analyze a set of diffuse reflection component based CSMs which are more compact than the three existing measures. The proposals for these measures are as follows:

Measure 13

$$S_{13} = 1 - \beta \arccos\left(\frac{\mathbf{x}_i \cdot \mathbf{x}_j}{\|\mathbf{x}_i\| \cdot \|\mathbf{x}_j\|}\right) \quad (5)$$

where $\beta > 0$ and $((S_{13} < 0) \Rightarrow (S_{13} = 0))$. $\beta = \frac{2}{\pi}$ is the special case where the largest possible angular difference would give a color similarity value of 0.

Measure 14

$$S_{14} = \exp\left(-\beta \left[1 - \frac{\mathbf{x}_i \cdot \mathbf{x}_j}{\|\mathbf{x}_i\| \cdot \|\mathbf{x}_j\|}\right]\right) \quad (6)$$

where $\beta > 0$.

[1] Note that the arguments $(\mathbf{x}_i, \mathbf{x}_j)$ are skipped in the formulae shown above and later on. Also note that the numbering of the measures is shown in accordance with the numbering used in [9, 10].

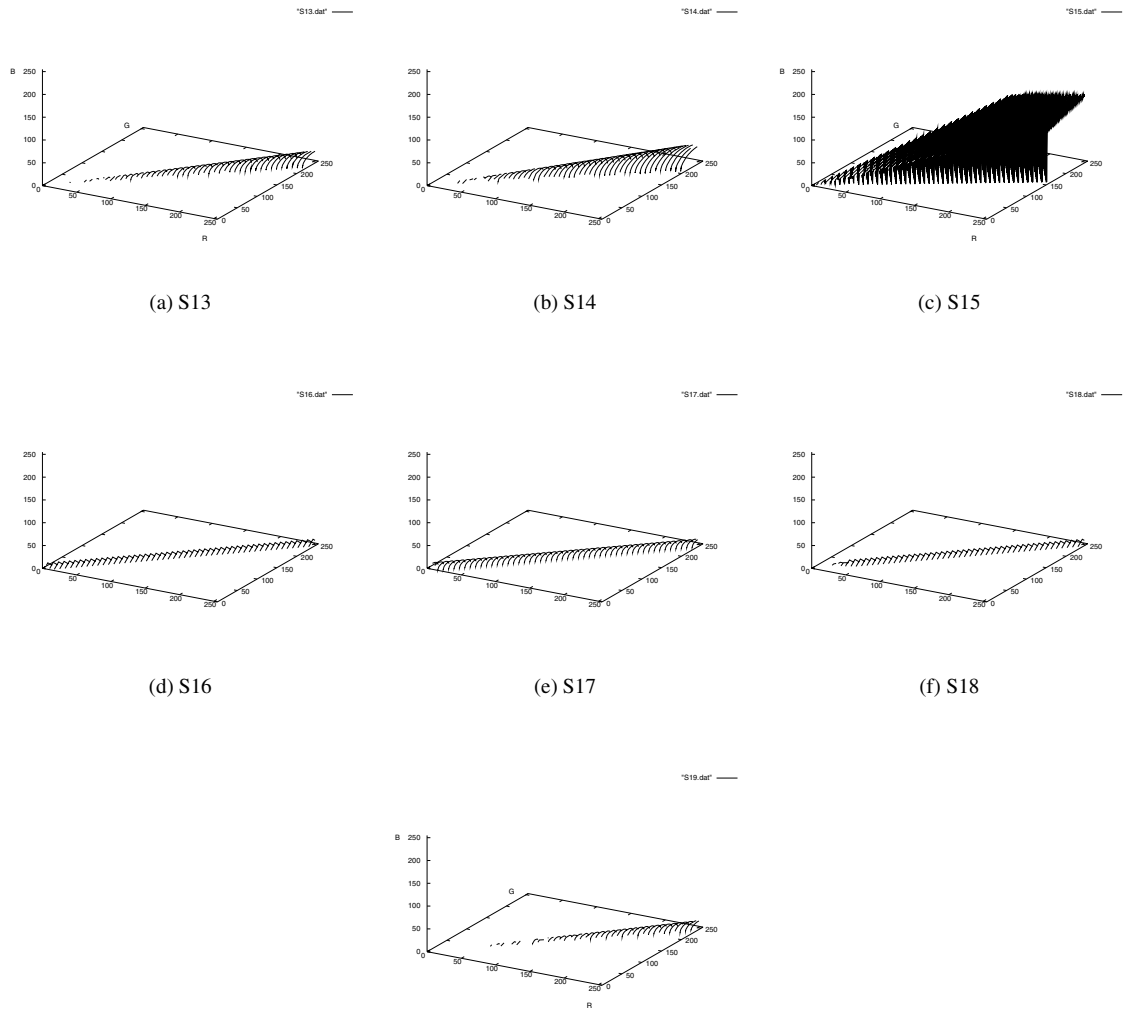

(a) S13 (b) S14 (c) S15

(d) S16 (e) S17 (f) S18

(g) S19

Figure 2: *Surfaces of similarity* $s = 0.80$ *for similarity measures* S_{13}, S_{14}, S_{15} *and* S_{16}. *(Surface for* S_{15} *is shown larger.)*

Measure 15

$$S_{15} = \exp\left(-\beta \sum_{k=1}^{p-1} \left| \frac{x_{ik}}{T_i} - \frac{x_{jk}}{T_j} \right| \right) \qquad (7)$$

where $\beta > 0$ and $T_i = \frac{1}{p}\sum_{k=1}^{p} x_{ik}$.

Measure 16

$$S_{16} = \exp\left(-\beta \left\| \frac{\mathbf{x}_i \cdot \mathbf{x}_j}{\mathbf{x}_j^2} \cdot \mathbf{x}_j - \mathbf{x}_i \right\| \right) \qquad (8)$$

where $\beta > 0$.

Measure 17

$$S_{17} = 1 - \beta \left\| \frac{\mathbf{x}_i \cdot \mathbf{x}_j}{\mathbf{x}_j^2} \cdot \mathbf{x}_j - \mathbf{x}_i \right\| \qquad (9)$$

where $\beta > 0$ and $((S_{17} < 0) \Rightarrow (S_{17} = 0))$.

Measure 18

$$S_{18} = \begin{cases} \exp\left(-\beta_1 \left[1 - \frac{\mathbf{x}_i \cdot \mathbf{x}_j}{\|\mathbf{x}_i\| \cdot \|\mathbf{x}_j\|}\right]\right), & \|\mathbf{x}_i\| < T \\ \exp\left(-\beta_2 \left\| \frac{\mathbf{x}_i \cdot \mathbf{x}_j}{\mathbf{x}_j^2} \cdot \mathbf{x}_j - \mathbf{x}_i \right\|\right), & \|\mathbf{x}_i\| \geq T \end{cases} \qquad (10)$$

Measure 19

$$S_{19} = \exp\left(-\beta \arccos\left(\frac{\mathbf{x}_i \cdot \mathbf{x}_j}{\|\mathbf{x}_i\| \cdot \|\mathbf{x}_j\|}\right)\right) \qquad (11)$$

where $\beta > 0$.

Figure 2 shows examples of constant similarity surfaces for similarity value $S = 0.8$ for all diffuse reflection component based CSMs proposed in this section.

S_{13} is a measure which computes the angle between the reference color and test color vectors in radians, scales it and subtracts the result from 1. S_{14} first subtracts the cosine of the angle between reference and test color vectors from 1 and uses the negated value as the argument of an exponential function. [2] The constant–similarity surfaces of both functions have the shape of cones, with vertices located at the origin of the color space coordinate system (see Fig.2(a) and (b)).

For S_{15}, first the chromaticity of both reference and test colors is computed by normalizing the color vectors with the colors' brightness values, and then the resulting $(p-1)$–dimensional vectors are used in the exponential function definition of S_8. [9, 10] The constant–similarity surface of this CSM turns out to have a complicated, irregular structure with many discontinuities (see Fig.2(c)).

Instead of CSMs with cone–shaped constant–similarity surfaces, CSMs with pipe–shaped constant–similarity surfaces can be defined; S_{16} and S_{17} are such measures, with the pipe of S_{16} having a rectangular cross–section and that of S_{17} having a circular cross–section. For these CSMs it must be kept in mind that $\mathbf{x}_i$ represents the reference color. The direction of the pipe is determined by the direction of the straight line through the reference color and the coordinate origin.

S_{18} is a combination of S_{14} and S_{16}. Its constant–similarity surface is cone–shaped for dark colors and pipe–shaped for bright colors. The switching brightness can be selected by setting the value of parameter T.

S_{19} is a measure which computes the angle between the reference color and test color vectors and uses it as the argument of the exponential function.

3.2. Selection of parameter β

All proposed reflection component based CSMs include a parameter β, the value of which should be selected such as to achieve optimal color separation of classes: Assuming only two color classes, the regions covered by these classes are manually extracted from several test images and the mean similarity between the color of class 1, m_1 (i.e. the reference color) and that of class 2, m_2, is computed for a range of β–values. The differences $\Delta m = m_1 - m_2$ as a function of the β–values can be shown to have a unique maximum, at which the optimal value for β is determined. The optimal values of β for each reflection component based CSM, obtained experimentally from real-world test images, are as follows: S_{13}: 3.5, S_{14}: 50.0, S_{15}: 12.0, S_{16}: 0.02, S_{17}: 0.02, S_{18}: 0.02 and 15.0, S_{19}: 6.0.

[2] Note that the exponential function was chosen because of the good results obtained for the point–type CSM S_8 reported in [9, 10].

4. Performance of reflection component based CSMs

4.1. Perceptual feature difference properties of CSM

Color similarity measures should be able to account for differences in the perceptual features hue, saturation and brightness in a balanced way. The functional relationship between differences in perceptual color feature values and color similarity values should be one-to-one and monotonic, and a reasonable value range of each of the perceptual features should map to the full range of color similarity values.

In order to examine the behavior of the CSMs with respect to saturation and hue changes, two sets of color vectors that are optimized for wide variation of saturation and hue values, respectively, were used as test data. Since diffuse reflection component based CSMs are insensitive to the brightness of a color, only results for saturation and hue are shown in Fig.3. The results of these tests can be summarized as follows:

- **Saturation**:
  1. The function $S_k(\Delta Sat)$ is neither 1-to-1 nor monotonic, but it maps the full range. This is true for S_{13}, S_{14}, S_{16}, S_{18} and S_{19}. An example is shown in Fig.3(a).
  2. The function $S_k(\Delta Sat)$ is 1-to-1, monotonic, and maps the full range. This is true for only S_{15} and S_{17}. An example is shown in Fig.3(c).
- **Hue**:
  1. Function $S_k(\Delta H)$ is neither 1-to-1 nor monotonic, but it maps the full range. This is true for only S_{15} (see Fig.3(d)).
  2. Function $S_k(\Delta H)$ is 1-to-1, monotonic, and maps full range. This is true for S_{13}, S_{14}, S_{16}, S_{17}, S_{18} and S_{19}. An example is shown in Fig.3(b).

All tested CSMs have quite similar behavior with respect to changes in saturation and hue. Measure S_{17} is closest to being ideal, and measure S_{16} has good properties, too.

4.2. Test results for class separation ability

A CSM is efficient in color classification tasks, if it has a good ability to separate color classes. More concretely, the mean similarity value $\bar{S}_m(i)$ in the image region of the i-th class and the mean color similarity value in the regions of other classes $\bar{S}_m(j)$ is required to differ as much as possible. That is, CSM S_k should be selected such that the difference

$$\bar{S}_k(i) - \bar{S}_k(j), i \neq j, \forall k \qquad (12)$$

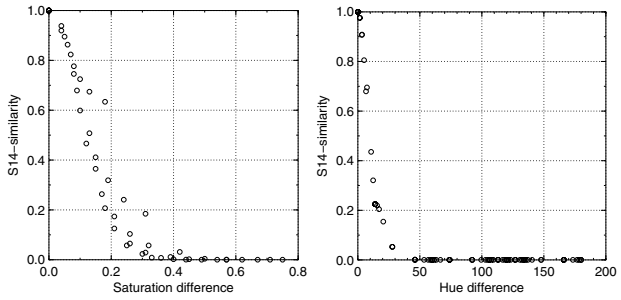

(a) S_{14} vs. Saturation difference

(b) S_{14} vs. Hue difference

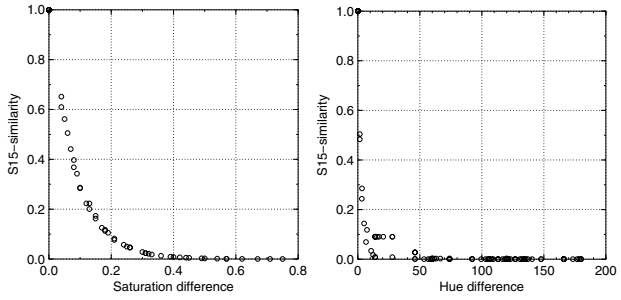

(c) S_{15} vs. Saturation difference

(d) S_{15} vs. Hue difference

Figure 3: *Typical examples of Similarity versus Saturation difference.*

is maximized, where k is the index identifying the CSMs.

In order to test the various color similarity measures with respect to their ability to separate color classes, we took a set of photographs of human faces with three types of CCD cameras (Sony XC003, Fujifilm FinePix 6900Z, Fujifilm Finepix 50i) and used them as test images in an experiment of human skin color classification. The test set included 55 images, taken in urban as well as natural outdoor environments, and office as well as private home indoor environments. Most images depict Asian nationals, and a few portray Europeans. All age groups are represented. The lighting conditions have not been controlled. Some sample images are shown in Fig.4.

Figure 4: *Examples of some of the face images used in the test.*

During the camera calibration stage, it was found that the transfer functions of the Fujifilm FinePix cameras were biased with approximately $\gamma = 2.0$. Consequently, all images taken by these cameras had to be corrected by a gamma–correction transformation applied to all three color components. This transformation was carried out such that no hue distortions occurred. The resulting images had properties as if they had been taken by cameras with linear transfer functions.

The facial skin regions were manually extracted from all 55 test images and saved as reference. The mean skin color of these reference regions were computed for each image and used as the skin reference color for the CSM. The similarity between this skin reference color and the colors of a given test image was computed at each pixel and for all diffuse reflection component based CSMs. Then, for each similarity image, the difference between mean similarities in the skin region, m_1, and in the non–skin region, m_2, were computed as $\Delta m = |m_1 - m_2|$. These results are shown in the diagram of Fig.5.

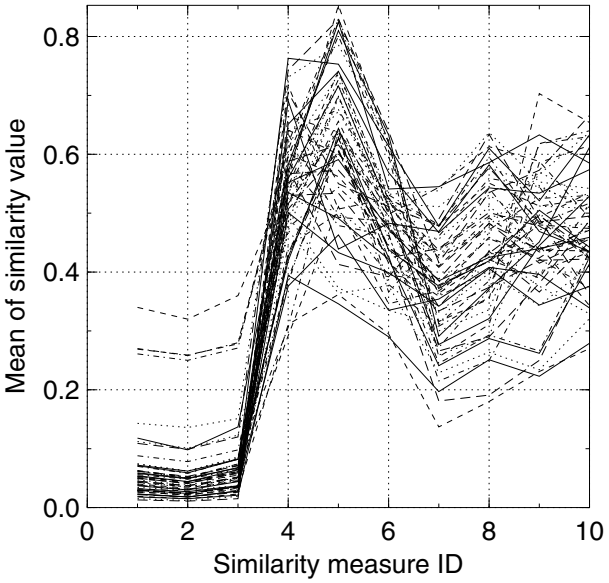

Figure 5: *Difference of mean similarity, $(m_2 - m_1)$, between face region and non-face region, for all color similarity measures and all test images. (Numbering on abscissa has the following meaning: $1 \rightarrow S_1$, $2 \rightarrow S_3$, $3 \rightarrow S_4$, $4 \rightarrow S_{13}$, $5 \rightarrow S_{14}$, $6 \rightarrow S_{15}$, $7 \rightarrow S_{16}$, $8 \rightarrow S_{17}$, $9 \rightarrow S_{18}$, $10 \rightarrow S_{19}$.)*

Fig.5 represents the graph for ΔS versus CSM ID number for all 55 test images. The difference in average similarity value between the skin region and other regions is clearly largest for measures S_{13} and S_{14}, followed by measures S_{15}, S_{19}, S_{18}, S_{17}, and S_{16}. The lowest differences are recorded for measures S_1, S_3 and S_4, which are the three CSMs included in the old set of color similarity measures. These data show that based on similarity values computed with S_{13} and S_{14}, facial skin color pixels can

be classified most efficiently. The high quality of the S_{14} measure is also obvious in the example of Fig.6.

(a) Original image. (b) S14 similarity image.

Figure 6: *Similarity image for facial skin color (gray–value is shown proportional to similarity value).*

4.3. Summary of results

With the exception of S_{15}, all proposed diffuse reflection component based CSMs are compact; S_{15} does not have smooth constant–similarity surfaces.

Regarding the behavior with respect to changes in saturation and hue, measures S_{16} and S_{17} are closest to being ideal, but the deviation of the other proposed CSMs from ideal behavior is only minor.

The test results for the CSMs' ability to separate color classes indicate that skin color pixels can be classified best when computation is based on S_{13} and S_{14}. It should be recalled that these two CSMs form cone–shaped constant–similarity surfaces in RGB color space, and the fact that they have the best ability to separate skin color from other colors is hardly surprising when considering that the distribution of skin colors in RGB color space is roughly cone–shaped, too. Since for S_{13} and S_{14} the similarity value difference exceeds 0.5, separation of skin color regions from non-skin color regions is easily achieved by discriminating the colors at an appropriately chosen similarity threshold value.

5. Conclusion

In this article we proposed several new color similarity measures for classifying colors that occur due to light reflection on object surfaces of the inhomogeneous dielectric materials type. The proposed measures are able to capture the similarity between the diffuse reflection components of colors. The results of an evaluation of the class separation ability of the diffuse reflection component based measures using more than 50 test images showed that the measures S_{13} and S_{14} perform best. The functional properties of all of these measures with respect to brightness, saturation and hue changes were found to be good.

References

[1] J. Hafner, H. S Sawhney, W. Equitz, M. Flickner and W. Niblack, Efficient Color Indexing for Quadratic Form Distance Functions, IEEE Trans. on Pattern Analysis and Machine Intelligence, Vol. 17, No. 7, 729-736 (1995)

[2] M. J. Swain and D. H. Ballard, Color Indexing, International Journal of Computer Vision, 7(1), 11-32 (1991)

[3] Y. Ohta, Knowledge-based Interpretation of Outdoor Natural Scenes, Pitman Publ. Inc., Marshfield, Mass. (1985).

[4] R. B. Ohlander and K. Price, Picture segmentation using a recursive region splitting method, Computer Vision and Image Processing, Vol. 8, No. 3 (1979).

[5] K. Nummiaro, E. Koller-Meier and L. Van Gool, Object tracking with an adaptive color-based particle filter, L. Van Gool(Ed.): Proc. of DAGM 2002, LNCS 2449, pp. 353-360 (2002).

[6] S. A. Shafer, "Using color to separate reflection components," Color Research and Applications, Vol. 10, 210-218 (1985)

[7] G. J. Klinker, S. A. Shafer, and T. Kanade, "The measurement of highlights in Color Images," International Journal of Computer Vision 2, 7-32 (1988)

[8] K. N. Plataniotis and A. N. Venetsanopoulos, Color Image Processing and Applications, Springer-Verlag, Berlin (2000)

[9] M. Hild and T. Emura, Which color similarity measure is most effective for background-frame differencing ?, Proc. 9th Color Imaging Conference, 168-173, Phoenix USA (2001)

[10] M. Hild, On the effectiveness of color similarity measures in background-frame differencing applications, Proc. of the First European Conference on Color in Graphics, Imaging and Vision, 304-309, Poitier, France (2002)